

Secondary frequency control with on-off load side participation in power networks

Andreas Kasis , Nima Monshizadeh and Ioannis Lestas

Abstract—We study the problem of secondary frequency regulation where ancillary services are provided via load-side participation. In particular, we consider on-off loads that switch when prescribed frequency thresholds are exceeded in order to assist existing secondary frequency control mechanisms. We show that system stability is not compromised despite the switching nature of the loads. However, such control policies are prone to Zeno-like behavior, which limits the practicality of these schemes. As a remedy to this problem, we propose a hysteretic on-off policy where loads switch on and off at different frequency thresholds. Moreover, we show that by exploiting appropriate decentralized passivity conditions, stability guarantees for a power network with hysteretic loads can be provided. Several relevant examples are discussed to demonstrate the applicability of the proposed results. Furthermore, numerical investigations of the results are provided on the Northeast Power Coordinating Council (NPCC) 140-bus system.

I. INTRODUCTION

It is anticipated that renewable sources of generation will increase their penetration in power networks in the near future [2], [3]. This is expected to introduce intermittency in the power generated resulting in additional challenges in the real time operation of power networks that need to be addressed.

A main objective in the operation of a power system is to ensure that generation matches demand in real time. This is achieved by means of primary and secondary frequency control schemes with the latter also ensuring that the frequency returns to its nominal value (50Hz or 60Hz). Secondary frequency control is traditionally performed by having the generation side following demand [4]. However, a large penetration of renewable sources of generation limits the controllability of generation and at the same time makes the system more sensitive to disturbances due to the reduced system inertia [5]. Controllable loads are considered by many a promising solution to counterbalance intermittent generation, being able to adapt their demand based on frequency deviations, providing fast response at urgencies. Recently, various research studies focused on the inclusion of controllable demand to aid both primary control as in [6]–[10] and secondary control as in [11], [12], [13].

Further from providing ancillary services at urgencies, it is also desired that controllable loads are non-disruptive, i.e. their assistance should have a negligible effect on users comfort, see e.g. [14]. Non-disruptive load-side control schemes ensure that loads alter their demand at urgencies but return to their normal operation when the danger for the network has been surpassed. Moreover, in many occasions, a realistic representation of loads involves only a discrete set of possible demand values, e.g. on and off states. Hence, incorporating on-off controllable loads that appropriately react to frequency deviations in power networks is of particular interest in load-side participation schemes.

Andreas Kasis and Nima Monshizadeh are with the Department of Engineering, University of Cambridge, Cambridge CB2 1PZ, UK; e-mails: ak647@cam.ac.uk, n.monshizadeh@eng.cam.ac.uk. Ioannis Lestas is with the Department of Engineering, University of Cambridge, and with the Cyprus University of Technology; email: icl20@cam.ac.uk.

A preliminary version of this work will appear in [1]. This manuscript includes the analytic proofs of the main results as well as additional results and discussion that demonstrate the applicability of the proposed analysis.

In this paper, we consider controllable on-off loads that switch when some frequency deviation is reached so that they assist the network at urgencies (i.e. when large frequency deviations are experienced) and otherwise return to their original operation. It will be shown that the inclusion of such loads does not compromise the stability of the power network, and results in enhanced frequency performance. However, it will be observed that such controllable loads may switch arbitrarily fast within a finite interval of time, or in other words, exhibit Zeno behavior. To avoid this phenomenon, we propose on-off loads with hysteretic dynamics where loads switch on and off at different frequency thresholds. As will be analytically shown, unlike (instantaneous) on-off loads, hysteretic loads do not induce Zeno behavior. Furthermore, we show that stability guarantees can be provided for the power network when hysteretic loads are employed. In particular, we allow general classes of higher order generation dynamics that satisfy a decentralized passivity condition [9], and prove stability of the network using Lyapunov approaches in conjunction with appropriate tools from nonsmooth analysis [15], [16]. Various examples are provided to demonstrate the applicability of the proposed results. Moreover, we provide a numerical validation of our results on the NPCC 140-bus system.

The structure of the paper is as follows: Section II includes some basic notation and preliminaries and in section III we present the power network model. In section IV we consider controllable demand that switches on/off whenever certain frequency thresholds are met and present our results concerning network stability. We also discuss in this section that problematic Zeno behaviour can be observed. In section V, we consider controllable loads with hysteretic patterns and show that the stability results extend to this case while avoiding the Zeno behaviour. In section VI we show how the results presented in Section V can be extended to include higher order dynamics for generation and demand that satisfy a passivity property. We also provide relevant examples that fit within the proposed framework. Numerical investigations of the results are provided in section VII. Finally, conclusions are drawn in section VIII.

II. NOTATION

Real numbers are denoted by \mathbb{R} , and the set of n -dimensional vectors with real entries is denoted by \mathbb{R}^n . The set of non-negative real numbers is denoted by $\mathbb{R}_{\geq 0}$. The set of natural numbers, including zero, is denoted by \mathbb{N}_0 . We use $\mathbf{0}_n$ to denote $n \times 1$ vector with all elements equal to 0. For a discrete set Σ , let $|\Sigma|$ denote its cardinality. For a set A , let $\bar{co}(A)$ denote its convex closure. For a point $x \in \mathbb{R}^n$ and constant $\delta > 0$ let $B(x, \delta)$ denote the ball of radius δ around x . Moreover, let $\mathcal{B}(\mathbb{R}^n)$ denote the collection of subsets of \mathbb{R}^n .

We use the notions of Lebesgue measurable set, zero measure set and Lebesgue measurable function from [17]. Furthermore, for a Lebesgue measurable set A , let $\mu(A)$ denote its Lebesgue measure. For notation convenience, Lebesgue measures will be referred to as just measures. When something holds almost everywhere within a measurable set A , it means that it holds everywhere in A except on sets N satisfying

$N \subset A : \mu(N) = 0$. For a set A and scalar b , $A \leq b$ denotes that all elements in A are less than or equal to b . Moreover, the function $\text{sgn}(x)$ takes a value of 1 when x is non-negative and -1 otherwise. The Laplace transform of a signal $h(t)$ is denoted by $\hat{h}(s) = \int_0^\infty e^{-st} h(t) dt$.

Within the paper a class of switching systems will be considered and the notion of Filippov solutions will be used for their analysis (see e.g. [16]). In particular, for any, potentially discontinuous, function $X : \mathbb{R}^n \rightarrow \mathbb{R}^n$, the Filippov set valued map $F[X] : \mathbb{R}^n \rightarrow \mathcal{B}(\mathbb{R}^n)$ is defined as,

$$F[X](x) \equiv \bigcap_{\delta > 0} \bigcap_{\mu(S)=0} \bar{co}(X(B(x, \delta) \setminus S)), x \in \mathbb{R}^n \quad (1)$$

where $\bigcap_{\mu(S)=0}$ denotes the intersection over all sets S of Lebesgue measure zero.

In order to facilitate the analysis of differential equations with discontinuous vector fields $X : \mathbb{R}^n \rightarrow \mathbb{R}^n$, the dynamical system below (a differential inclusion) is often considered

$$\dot{x}(t) \in F[X](x(t)). \quad (2)$$

For systems described by (2), a Filippov solution is defined as an absolutely continuous map $x : [0, t_1] \rightarrow \mathbb{R}^n$ that satisfies (2) for almost all $t \in [0, t_1]$. For the system that will be studied in the paper we will show that Filippov solutions exist and are unique.

Note that the use of Filippov solutions allows the study of systems with discontinuous dynamics when there are infinitely many switches at finite time, a phenomenon known as Zeno behavior (see Remark 2).

III. NETWORK MODEL

We describe the power network model by a connected graph (N, E) where $N = \{1, 2, \dots, |N|\}$ is the set of buses and $E \subseteq N \times N$ the set of transmission lines connecting the buses. Furthermore, we use (i, j) to denote the link connecting buses i and j and assume that the graph (N, E) is directed with arbitrary orientation, so that if $(i, j) \in E$ then $(j, i) \notin E$. For each $j \in N$, we use $i : i \rightarrow j$ and $k : j \rightarrow k$ to denote the sets of buses that are predecessors and successors of bus j respectively. It is important to note that the form of the dynamics in (3)–(4) below is unaltered by any change in the graph ordering, and all of our results are independent of the choice of direction. The following assumptions are made for the network:

- 1) Bus voltage magnitudes are $|V_j| = 1$ p.u. for each $j \in N$.
- 2) Lines $(i, j) \in E$ are lossless and characterized by their susceptances $B_{ij} = B_{ji} > 0$.
- 3) Reactive power flows do not affect bus voltage phase angles and frequencies.

We use swing equations, see e.g. [18], to describe the frequency dynamics at each bus:

$$\dot{\eta}_{ij} = \omega_i - \omega_j, (i, j) \in E, \quad (3a)$$

$$M_j \dot{\omega}_j = -p_j^L + p_j^M - (d_j^c + d_j^u) - \sum_{k:j \rightarrow k} p_{jk} + \sum_{i:i \rightarrow j} p_{ij}, j \in N, \quad (3b)$$

$$p_{ij} = B_{ij} \sin \eta_{ij}, (i, j) \in E. \quad (3c)$$

In system (3), the time-dependent variables p_j^M , d_j^c and ω_j represent, respectively, the mechanical power injection, the frequency dependent controllable load and the deviation from the nominal¹ frequency at bus j . The quantity d_j^u is also

a time-dependent variable that represents the uncontrollable frequency-dependent load and generation damping present at bus j . Furthermore, the quantities η_{ij} and p_{ij} are time-dependent variables that represent, respectively, the power angle difference, and the power transmitted from bus i to bus j . The constant $M_j > 0$ denotes the generator inertia, and the constant p_j^L denotes the frequency-independent load at bus j . We study the response of system (3) for a step change in the frequency independent uncontrollable demand p_j^L at each bus.

A. Generation and frequency-dependent load dynamics

We shall consider generation dynamics and frequency-dependent loads given by

$$\dot{p}_j^M = -\alpha_j \omega_j, j \in N, \quad (4a)$$

$$d_j^u = A_j \omega_j, j \in N, \quad (4b)$$

where $A_j > 0$ and $\alpha_j \geq 0$ for all $j \in N$. We assume that there exists at least one bus equipped with the integral controller above, i.e. $\max_{j \in N} (\alpha_j) > 0$. In case $\alpha_j = 0$, the generation output is equal to a constant, namely $p_j^M = p_j^{M,*}$.

Remark 1: The restriction to the class of PI controllers (4) with turbine governor dynamics omitted is merely for the sake of simplicity, and is made in order to keep the focus on loads with on-off behavior. In section VI we show how more complex control schemes and high order generation/demand dynamics can be accommodated in our setup.

Next, we will consider two classes of decentralized control schemes for discrete loads that provide ancillary services to the power network in the secondary control time-frame and investigate their performance and stability properties. As it will be discussed within the paper, the discrete character of the loads leads to discontinuous system dynamics that can introduce additional complications that need to be explicitly addressed.

IV. LOADS WITH SWITCHING

A. Problem formulation

In this section, we consider frequency dependent on-off loads that respond to frequency deviations by switching to an appropriate state in order to aid the network at urgencies. As the network returns to its normal operating conditions, the loads return to their initial state as well, hence affecting users comfort for short periods only. In particular, for each² $j \in N$, we consider the following switching dynamics for the controllable loads:

$$d_j^c(\omega_j) = \begin{cases} \bar{d}_j, & \omega_j > \bar{\omega}_j, \\ 0, & \underline{\omega}_j < \omega_j \leq \bar{\omega}_j, \\ \underline{d}_j, & \omega_j \leq \underline{\omega}_j, \end{cases} \quad (5)$$

where $-\infty < \underline{d}_j \leq 0 \leq \bar{d}_j < +\infty$, and $\bar{\omega}_j > 0 > \underline{\omega}_j$. The dynamics in (5) are depicted on Figure 1. Note that these dynamics can be trivially extended to include more discrete values, that would possibly respond to higher frequency deviations.

¹The nominal value of frequency is equal to 50Hz (or 60Hz).

²This can be trivially relaxed to any subset of N .

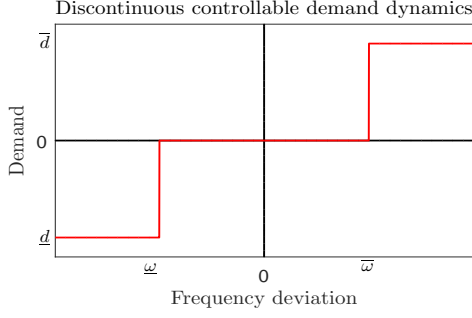


Fig. 1. Switch dynamics for controllable loads as described by (5).

To cope with the switching dynamics of the loads, and to have well-defined solutions to system (5) for all time, we first define a Filippov set valued map as follows:

$$F[d_j^c] = \begin{cases} \{\bar{d}_j\}, & \omega_j > \bar{\omega}_j, \\ [0, \bar{d}_j], & \omega_j = \bar{\omega}_j \\ \{0\}, & \underline{\omega}_j < \omega_j < \bar{\omega}_j, \quad j \in N. \\ [\underline{d}_j, 0], & \omega_j = \underline{\omega}_j, \\ \{\underline{d}_j\}, & \omega_j < \underline{\omega}_j, \end{cases} \quad (6)$$

The state of the interconnected system (3)–(5) is denoted by $x = (\eta^T, \omega^T, (p^M)^T)^T$, where any variable without subscript represents a vector with all respective components. For a compact representation of the system, we consider the Filippov set valued map $Q : \mathbb{R}^n \rightarrow \mathcal{B}(\mathbb{R}^n)$, with $n = |E| + 2|N|$, and write the system dynamics as the following differential inclusion:

$$\dot{x} \in Q(x) \quad (7)$$

where

$$Q(x) = \begin{cases} \{\omega_i - \omega_j\}, (i, j) \in E, \\ \left\{ \frac{1}{M_j}(-p_j^L + p_j^M - A_j \omega_j - v_j - \sum_{k:j \rightarrow k} p_{jk}) \right. \\ \left. + \sum_{i:i \rightarrow j} p_{ij} \right\} : v_j \in F[d_j^c], j \in N, \\ \{-\alpha_j \omega_j\}, j \in N. \end{cases}$$

Remark 2: As a result of the switching dynamics in (5), the vector field in (3b) will become discontinuous. This discontinuity limits the applicability of classical solutions to the ordinary differential equations (3), and asks for an appropriate notion of solutions. The most suitable notion depends on the objective and the problem at hand. Among several solution notions, see [19], we opt for Filippov solutions [14] which amounts to the relaxation of the differential equation to a differential inclusion, see (7). The idea behind Filippov solutions is to study the behavior of the vector field *around* a point of discontinuity, and consequently allow the vector field to take any value within an admissible set. As will be observed in Lemma 2, this does not spoil uniqueness of solutions for the dynamics considered in this paper.

B. Equilibria, existence and uniqueness of solutions

The discontinuous dynamics (5) introduce additional complexity in the analysis of the behavior of (7). First, we study equilibria of the system, and then investigate existence and uniqueness of Filippov solutions. An equilibrium of (7) is defined as follows:

Definition 1: The point $x^* = (\eta^*, \omega^*, p^{M,*})$ defines an equilibrium of the system (7) if $0_n \in Q(x^*)$.

At an equilibrium of the system, the controllable demand takes its value from a set that depends on ω_j^* , i.e., $d_j^{c,*} \in F[d_j^c](\omega_j^*)$, $j \in N$. Lemma 1 below, proven in the supplementary material, shows that this set is singleton, namely $Q(x^*) = \{0_n\}$, and $\omega^* = 0_{|N|} = d_j^{c,*}$.

Lemma 1: For any equilibrium point $x^* = (\eta^*, \omega^*, p^{M,*})$ of (7), we have $\omega^* = 0_{|N|}$ and $Q(x^*) = \{0_n\}$.

It should further be noted that within the rest of the paper the existence of some equilibrium of (7) is assumed. As evident from Lemma 1, the conditions for existence of an equilibrium can be studied independent of the switching loads, see e.g. [20].

In addition, we impose a constraint on the differences of the phase angles at the equilibrium. This assumption, stated below, is ubiquitous in power network literature, and is treated as a security constraint.

Assumption 1: $|\eta_{ij}^*| < \frac{\pi}{2}$ for all $(i, j) \in E$.

The following lemma, proven in the supplementary material, establishes existence and uniqueness of solutions to (3)–(5).

Lemma 2: There exists a unique Filippov solution of (3)–(5) starting from any initial condition $x_0 = (\eta(0), \omega(0), p^M(0)) \in \mathbb{R}^n$.

C. Stability

We now state the main result of this section, proven in the supplementary material:

Theorem 1: Suppose that there exists an equilibrium $(\eta^*, \omega^*, p^{M,*})$ of (7) for which Assumption 1 is satisfied. Then there exists an open neighborhood Ξ of this equilibrium such that Filippov solutions (η, ω, p^M) of (7) starting in this region asymptotically converge to the set of equilibria of the system. In particular, the frequency vector ω converges to $\omega^* = 0_{|N|}$.

The theorem above establishes stability of the power network (3)–(4) with on-off load control (5), and shows that frequency is restored to its nominal value after a transient load-side participation.

D. Zeno behavior

A possible feature of switching and hybrid systems is the occurrence of infinitely many switches within some finite time, a phenomenon known as Zeno behavior (e.g. [15]). Such behavior is often undesirable and impedes practical implementations.

In our setting, Zeno behavior may occur in on-off loads as shown numerically in Section VII. The reason such behavior may occur is that the frequency derivative may change sign when passing a discontinuity, causing the vector field to point towards the discontinuity. For instance, suppose that $0 < \dot{\omega}_j(t_1) < \bar{d}_j$ for some time instant $t_1 > 0$, and that the threshold $\bar{\omega}_j$ is met at this time. Then, the load d_j^c switches on, causing a sign change in the value of $\dot{\omega}_j$. Hence, the frequency vector field will point at a direction of frequency decrease that will force the load to switch off. These on/off switches occur infinitely many times in a finite time, resulting in the aforementioned Zeno behavior. Note that this phenomenon is only observed here during the transient response of the loads, as the mechanical power injection (4) will eventually dictate the sign of the vector field and regulate the frequency to its nominal value as shown in Theorem 1.

V. HYSTERESIS ON CONTROLLABLE LOADS

A. Problem formulation

In this section, we propose the use of hysteretic dynamics in on-off controllable loads, which means that a controllable

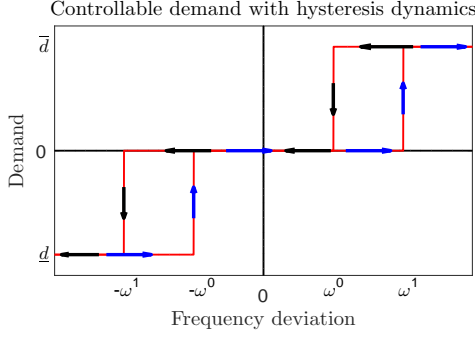


Fig. 2. Hysteresis dynamics for controllable loads as described by (8).

load switches on and off at different frequency thresholds. As will be observed, this modification will ensure that the system does not exhibit Zeno behavior. For relevant applications of hysteric dynamics in ruling out chattering, Zeno behavior, and other undesired features, see. e.g. [21]–[23].

We consider the following hysteretic dynamics for controllable loads:

$$d_j^c = \bar{d}_j \sigma_j \quad (8a)$$

$$\sigma_j(t^+) = \begin{cases} \text{sgn}(\omega_j), & |\omega_j| \geq \omega_j^1 \\ 0, & |\omega_j| \leq \omega_j^0 \\ \sigma_j(t), & \text{otherwise} \end{cases} \quad (8b)$$

where $j \in N$, $t^+ = \lim_{\epsilon \rightarrow 0} (t + \epsilon)$, and the frequency thresholds ω_j^0, ω_j^1 , satisfy $\omega_j^1 > \omega_j^0 > 0$.

The dynamics described in (8) are depicted in Figure 2. Note that σ_j takes its value from the set $P = \{-1, 0, 1\}$.

Now the behavior of the system (3),(4),(8), can be described by the states $z = (x, \sigma)$, where $x = (\eta, \omega, p^M) \in \mathbb{R}^n$ is the continuous state, and $\sigma \in P^{|N|}$ the discrete state. The domain of solution is then equal to $\mathbb{R}^n \times P^{|N|}$, which we denote in short by Λ .

The continuous part of the dynamics (3),(4),(8), is given by

$$\dot{\eta}_{ij} = \omega_i - \omega_j, \quad (i, j) \in E, \quad (9a)$$

$$M_j \dot{\omega}_j = -p_j^L + p_j^M - (\bar{d}_j \sigma_j + A_j \omega_j) - \sum_{k:j \rightarrow k} p_{jk} + \sum_{i:i \rightarrow j} p_{ij}, \quad j \in N, \quad (9b)$$

$$p_{ij} = B_{ij} \sin \eta_{ij}, \quad (i, j) \in E, \quad (9c)$$

$$\dot{p}_j^M = -\alpha_j \omega_j, \quad j \in N, \quad (9d)$$

$$\dot{\sigma}_j = 0, \quad j \in N, \quad (9e)$$

This is valid when z belong to the set

$$C = \{z \in \Lambda : \sigma_j \in \mathcal{I}_j(\omega_j), \forall j \in N\} \quad (10)$$

where

$$\mathcal{I}_j(\omega_j) = \begin{cases} \{\text{sgn}(\omega_j)\}, & |\omega_j| \geq \omega_j^1, \\ \{0\}, & |\omega_j| \leq \omega_j^0, \\ \{0, \text{sgn}(\omega_j)\}, & \omega_j^0 < |\omega_j| < \omega_j^1. \end{cases}$$

Alternatively, when $z \in \Lambda \setminus C$, the system dynamics evolve according to the following discrete update rule:

$$x^+ = x \quad (11)$$

$$\sigma_j(t^+) = \begin{cases} \text{sgn}(\omega_j), & |\omega_j| \geq \omega_j^1 \\ 0, & |\omega_j| \leq \omega_j^0 \end{cases}$$

where the latter is in agreement with (8b). We can now provide the following compact representation for the hybrid system (3),(4),(8),

$$\dot{z} = f(z), \quad z \in C, \quad (12a)$$

$$z^+ = g(z), \quad z \in D, \quad (12b)$$

where C is given by (10), $D = \Lambda \setminus C$, and $z^+ = z(t^+)$. The maps $f(z) : C \rightarrow \Lambda$ and $g(z) : D \rightarrow C$ are given by (9) and (11), respectively. Note that $z^+ = g(z)$ represents a discrete dynamical system where z^+ is determined by the current value of the state z and the update rule given by g .

We assume that the initial conditions are compatible with (12), or essentially with the transition map in (8b). This means that, for each $j \in N$, $\sigma_j(0) \in \bar{\mathcal{I}}_j(\omega_j(0))$ where

$$\bar{\mathcal{I}}_j(\omega_j) = \begin{cases} \{\text{sgn}(\omega_j)\}, & |\omega_j| > \omega_j^1 \\ \{0\}, & |\omega_j| < \omega_j^0 \\ \{0, \text{sgn}(\omega_j)\}, & \omega_j^0 \leq |\omega_j| \leq \omega_j^1. \end{cases} \quad (13)$$

We write the condition above in vector form as $\sigma(0) \in \bar{\mathcal{I}}(\omega(0))$, and we denote the set of compatible initial conditions by $\Lambda_0 \subseteq \Lambda$.

B. Analysis of equilibria and solutions

Before investigating stability of the hybrid system in (12), we characterize its equilibria, and establish existence and uniqueness of solutions.

Note that we call a point $z^* = (x^*, \sigma^*)$ an equilibrium of (12) if $f(z^*) = 0$, $z^* \in C$ or $z^* = g(z^*)$, $z^* \in D$. Now, we state the following lemma:

Lemma 3: For any equilibrium point $z^* = (x^*, \sigma^*)$ of (12), we have $\omega^* = \sigma^* = \mathbf{0}_{|N|}$. Moreover, $z^* \in C$.

To proceed further, we need to assume existence of some equilibrium of (12). As evident from Lemma 3, the feasibility of this assumption is independent of the on-off loads and has been studied in literature (e.g. [20]).

Following [15], [23], we define a hybrid time domain K as a subset of $\mathbb{R}_{\geq 0} \times \mathbb{N}_0$ consisting of, potentially infinite, time intervals of the form $[t_\ell, t_{\ell+1}] \times \{\ell\}$, where $\ell = 0, 1, 2, \dots$. Accordingly, a solution of a hybrid system is given by a function $z(t, \ell)$ defined on a hybrid time domain such that $z(t, \ell) \in C$ and $\dot{z} = f(z)$ for all $t \in [t_\ell, t_{\ell+1}]$, and $z(t_{\ell+1}, \ell + 1) = g(z(t_{\ell+1}, \ell))$ for $z(t_{\ell+1}, \ell) \in D$. A solution $z(t, \ell)$ is complete if its corresponding time domain is unbounded. A solution is maximal if it cannot be extended (detailed definitions are provided in section B of the supplementary material).

For convenience in the presentation we will refer to maximal solutions by just solutions. Existence and uniqueness of solutions to (12) are established in the following lemma.

Lemma 4: There exists a complete unique solution $z = (x, \sigma)$ to (12), starting from any initial condition $z(0, 0) \in \Lambda_0$.

Furthermore, the following proposition shows the existence of some finite dwell time between switches of states σ_j for any bounded solution. Within it, we denote the time-instants where the value of σ_j changes by $t_{\ell, j}$, $\ell \in \mathbb{N}_0, j \in N$.

Proposition 1: For any complete bounded solution of (12), there exists $\tau_j > 0$ such that $\min_{\ell \geq 1} (t_{\ell+1, j} - t_{\ell, j}) \geq \tau_j$ for any $j \in N$.

Remark 3: The importance of Proposition 1 is that it shows that no Zeno behavior will occur for any complete bounded solution of system (12). This is because for any finite time interval $\tau = \min_j \tau_j$, $j \in N$, the vector σ changes at most $|N|$ times. This highlights the practical advantage of (12) compared to (7). This analytic result is verified by numerical simulations in a realistic power network, as discussed in section VII.

C. Stability of hysteresis system

Now, we are at the position to state the stability result concerning the system (12).

Theorem 2: Let $z^* = (x^*, \sigma^*)$, with $\omega^* = \sigma^* = 0_{|N|}$, be an equilibrium of (12) for which Assumption 1 holds. Then there exists an open neighborhood S of x^* such that solutions $z = (x, \sigma)$, with $x(0) \in S$ and $\sigma(0) \in \bar{\mathcal{I}}(\omega(0))$, asymptotically converge to the set of equilibria of (12). In particular, the vectors ω and σ converge to the vector $0_{|N|}$.

Remark 4: Theorem 2 shows that the hysteretic dynamics in (8) do not compromise the stability of the system. This, together with the absence of Zeno behavior shown in Proposition 1, promotes the use of hysteretic dynamics as a means to provide practical and non-disruptive on-off load side control to the power network.

Remark 5: Although the controllable loads do not participate at the equilibrium, they provide ancillary services to the network, and improve the performance in transient time. This is numerically investigated in Section VII. To clarify, note that the convergence region in Theorem 2 is not restricted by the switches, but rather by the nonlinearity of the frequency dynamics.

VI. PASSIVE CONTINUOUS DYNAMICS

In this section, we extend the scope of the results by considering a general class of continuous nonlinear dynamics for generation and demand. The relevance and generality of this class of dynamics will be demonstrated with various examples. We opt for the hysteretic load setting described in (8) rather than the switching loads given by (5) to avoid possible Zeno behaviour.

A. Dynamics for generation and demand

For convenience in the analysis, we define a net power supply variable s_j that represents the aggregation of continuous generation and demand at bus j , given by

$$s_j = p_j^M - d_j^u, j \in N. \quad (14)$$

To incorporate general classes of dynamics for the net supply variables, we assume that s_j is the output of a nonlinear system, namely

$$\dot{x}_j^s = f_j(x_j^s, -\omega_j), \quad (15a)$$

$$s_j = g_j(x_j^s, -\omega_j), \quad (15b)$$

for each $j \in N$. Here, $x_j^s \in \mathbb{R}^{n_j}$, with $n_j \in \mathbb{N}_0$, is the state of the system, and $f_j : \mathbb{R}^{n_j} \times \mathbb{R} \rightarrow \mathbb{R}^{n_j}$, and $g_j : \mathbb{R}^{n_j} \times \mathbb{R} \rightarrow \mathbb{R}$ are globally Lipschitz for each $j \in N$. We assume the existence of an equilibrium for the system (15a) when $\omega_j = 0$, i.e. that there exists $x_j^{s,*}$ such that $f_j(x_j^{s,*}) = 0$. Moreover, for a constant input $-\omega_j = -\bar{\omega}_j$, we assume that $\dot{x}_j^s = f_j(x_j^s, -\bar{\omega}_j)$ has no invariant set other than equilibrium points. For a linear system, this means that the state matrix has all its eigenvalues in the open left half plane, except from a possible single eigenvalue at the origin.

Furthermore, the following assumption ensures that at equilibrium, frequency will be at its nominal value.

Assumption 2: There exists at least one bus j such that the dynamics in (15a) satisfy $f_j(\bar{x}_j^s, -\bar{\omega}_j) = 0$, for some constants $\bar{\omega}_j$ and \bar{x}_j^s , only if $\bar{\omega}_j = 0$.

Remark 6: Assumption 2 requires that for at least one bus, the dynamics are such that an equilibrium can be reached only if the frequency is at its nominal value. Such requirement is satisfied if a control policy with integral action is used as in

(4), and the more general schemes discussed in Section VI-D. Moreover, note that Assumption 2 needs not to be satisfied by all buses. This reflects the fact that traditionally secondary control is performed by a small number of buses, where the rest may only provide support at faster timescales without incorporating integral action.

The final condition that we impose on the dynamics in (15) is related to a notion of passivity that is discussed next.

Definition 2: The system (15) is said to be locally input strictly passive about the constant input $-\bar{\omega}_j$ and the point \bar{x}_j^s if there exist open neighborhoods Ω_j of $-\bar{\omega}_j$ and X_j^s of \bar{x}_j^s and a continuously differentiable positive definite function $V_j^S(x_j^s)$ (called the storage function) with a strict minimum at $x_j^s = \bar{x}_j^s$, such that, for all $-\omega_j \in \Omega_j$ and all $x_j^s \in X_j^s$,

$$\dot{V}_j^S(x_j^s) \leq (-\omega_j + \bar{\omega}_j)(s_j - \bar{s}_j) - \phi_j(-\omega_j + \bar{\omega}_j), \quad (16)$$

where ϕ_j is a positive definite function and $\bar{s}_j = g_j(\bar{x}_j^s, -\bar{\omega}_j)$.

We now suppose that the power supply variables at each bus satisfy this input strict passivity condition about the equilibrium.

Assumption 3: For each $j \in N$, the dynamics (14) are locally input strictly passive about the constant input $-\omega_j^*$ and an equilibrium $x_j^{s,*}$, in the sense of Definition 2.

Remark 7: Assumption 3 is a decentralized condition on the continuous power supply dynamics that allows to deduce stability guarantees over a broad range of dynamics. This assumption holds for many dynamical systems considered in the literature and allows the inclusion of higher order schemes (see also [9] and the discussion within it). In Section VI-D, we provide various relevant examples that satisfy Assumption 3 to demonstrate its practicality within the considered secondary frequency control setting.

B. Hybrid system representation

In this section, we provide a compact mathematical formulation of the system described by (3), (8), (14), (15) that is useful in the subsequent analysis. To study the behavior of this system, we define the states $z = (x, \sigma)$, where $x = (\eta, \omega, x^s)$ is the continuous state and σ the discrete state, similarly to Section V. Furthermore, we use $\bar{\Lambda} \subset \mathbb{R}^m \times P^{|N|}$, where $m = |E| + |N| + \sum_{j \in N} n_j$, to denote the domain of solutions of the considered system.

The dynamics of (3), (8), (14), (15) can be described by the following compact hybrid representation:

$$\dot{z} = f(z), z \in C, \quad (17a)$$

$$z^+ = g(z), z \in D, \quad (17b)$$

where g and C are as depicted in (10) and (11) respectively, $D = \bar{\Lambda}/C$ and f is described by

$$\dot{\eta}_{ij} = \omega_i - \omega_j, (i, j) \in E, \quad (18a)$$

$$M_j \dot{\omega}_j = -p_j^L + s_j - (\bar{d}_j \sigma_j) - \sum_{k: j \rightarrow k} p_{jk} + \sum_{i: i \rightarrow j} p_{ij}, \quad (18b)$$

$$p_{ij} = B_{ij} \sin \eta_{ij}, (i, j) \in E, \quad (18c)$$

$$\dot{x}_j^s = f_j(x_j^s, -\omega_j), \quad s_j = g_j(x_j^s, -\omega_j), \quad j \in N, \quad (18d)$$

$$\dot{\sigma}_j = 0, \quad j \in N \quad (18e)$$

Similarly to Section V we assume that the initial conditions are compatible to (17) which means that $\sigma_j(0) \in \bar{\mathcal{I}}_j(\omega_j(0))$, $j \in$

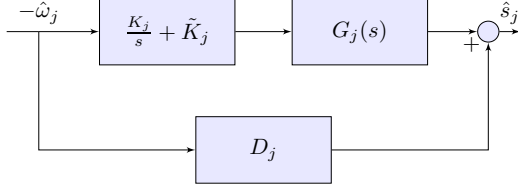


Fig. 3. Laplace domain representation of frequency dependent power supply variable consisting of the summation of a term corresponding to the system damping, and the series interconnection of a linear system with a proportional integral controller.

N , where \bar{I}_j is as described by (13). We denote the set of compatible initial conditions of (17) by $\bar{\Lambda}_0 \subseteq \bar{\Lambda}$.

The following lemma, proven in the supplementary material, shows that the equilibrium frequency of (17) is the same as the nominal, when Assumption 2 holds. This shows that the considered setting satisfies the secondary frequency control requirements.

Lemma 5: Consider (17) and let Assumption 2 hold. Then, any equilibrium point $z^* = (x^*, \sigma^*)$ of (17) satisfies $\omega^* = \sigma^* = 0_{|N|}$. Moreover, $z^* \in C$.

C. Main results

We are now in a position to extend our main results to include the class of power supply dynamics described in section VI-A. First, in order to ensure that the presented hybrid mathematical formulation is suitable to describe a realistic system, we note that there exists a complete unique solution $z = (x, \sigma)$ to (17), starting from any initial condition $z(0, 0) \in \bar{\Lambda}_0$. This follows directly from the proof of Lemma 4 and the fact that the vector field f , described by (18) is Lipschitz continuous.

Furthermore, the existence of some finite dwell time between consecutive switches of states σ_j for any bounded solution can be demonstrated in analogy to Proposition 1, as follows from the Lipschitz continuity of frequency variables in (18b).

The convergence of solutions to (17) to an equilibrium that satisfies the requirements of secondary control is stated in the following theorem, proven in the supplementary material.

Theorem 3: Let $z^* = (x^*, \sigma^*)$, with $\omega^* = \sigma^* = 0_{|N|}$, be an equilibrium of (17) for which Assumptions 1–3 hold. Then there exists an open neighborhood S of x^* such that solutions $z = (x, \sigma)$, with $x(0) \in S$ and $\sigma(0) \in \bar{\mathcal{I}}(\omega(0))$, asymptotically converge to the set of equilibria of (17). In particular, the vectors ω and σ converge to the vector $0_{|N|}$.

Remark 8: Theorem 3 demonstrates the local convergence of solutions to the hybrid system (17). It extends Theorem 2 by incorporating a broad class of continuous generation and demand dynamics that are relevant in power networks, as shown in Subsection VI-D below. Hence, the results presented in this section demonstrate that hysteretic controllable loads can be present in a power network with passive continuous power supply dynamics without compromising stability nor inducing undesirable performance effects such as Zeno behavior.

D. Discussion

To demonstrate the generality and applicability of the conditions presented in Section VI-A, we devote this section to discuss various examples that fit within the proposed framework.

Further to the proportional-integral generation and demand dynamics described in Section III-A, our analysis allows to consider the general class of dynamics depicted in Figure 3,

where power supply dynamics are described by the summation of a damping term and the linear interconnection of a PI controller with an asymptotically stable general linear system³, potentially of higher order. The transfer function from $-\omega_j$ to s_j of such a system is given by $S_j(s) = (\frac{K_j}{s} + \tilde{K}_j)G_j(s) + D_j$. Assumption 2 and the assumptions on (15a), (15b), are clearly satisfied for this system. Moreover, Assumption 3 is satisfied if there exists $\epsilon_j > 0$ such that the perturbed transfer function $S_j(s) - \epsilon_j$ is positive real. This can be numerically verified with appropriate LMI (Linear Matrix Inequality) conditions [24, Lemma 6.2], i.e. a computationally efficient convex feasibility problem, or graphically by examining the Nyquist plot of $\hat{S}_j(j\omega)$, which needs to lie within the open right half plane.

First, we consider power supply dynamics where the output response follows from a PI control scheme acting on a frequency input with a lag. Such dynamics can be described by

$$\dot{\alpha}_j = -K_j\omega_j, \quad \tau_{\beta,j}\dot{\beta}_j = -\beta_j + \alpha_j - \tilde{K}_j\omega_j, \quad (19a)$$

$$s_j = \beta_j - D_j\omega_j, \quad (19b)$$

where α_j, β_j are the states of the power supply variables and $K_j, \tilde{K}_j, \tau_{\beta,j}, D_j$ are positive constants describing the integrator and droop gains, the time constant associated with power generation and the frequency damping respectively. For (19), it can be shown that Assumption 3 is satisfied if $K_j\tau_{\beta,j} < D_j + \tilde{K}_j$. Furthermore, Assumption 2 is trivially satisfied.

An important aspect of our analysis lies in its ability to consider higher order schemes. A significant example of this can be seen in second order generation dynamics, often considered to describe turbine-governor behaviour (e.g. [18]). Below, we consider the series interconnection of an integrator and a second order system with some frequency damping, described by

$$\dot{\alpha}_j = -K_j\omega_j, \quad \tau_{\beta,j}\dot{\beta}_j = -\beta_j + \alpha_j, \quad (20a)$$

$$\tau_{\gamma,j}\dot{\gamma}_j = -\gamma_j + \beta_j, \quad s_j = \gamma_j - D_j\omega_j, \quad (20b)$$

where $\alpha_j, \beta_j, \gamma_j$ are internal states of the system and $K_j, \tau_{\beta,j}, \tau_{\gamma,j}, D_j$ positive constants. It is straightforward to deduce that such system satisfies Assumption 2. Furthermore, it can be shown that (20) satisfies Assumption 3 when $K_j(\tau_{\beta,j} + \tau_{\gamma,j}) < D_j$.

The Nyquist plots for systems (19) and (20), when their respective gain conditions are marginally satisfied, are illustrated on Figure 4 which demonstrates the passivity of both schemes, implied from the fact that both plots are on the right half plane.

Furthermore, our framework allows to incorporate various realistic dynamical schemes that satisfy Assumption 3, but not Assumption 2. This is relevant since Assumption 2 needs to be satisfied by at least one bus in the network, and reflects the fact that traditionally secondary control is performed by only a small number of buses, where the rest often contribute at faster timescales associated with primary control. To demonstrate an important example of such a case, we consider the fifth order dynamics used by the Power System Toolbox [25] to describe turbine governor behavior within the NPCC network. In this model, power supply \hat{s}_j is related to the negative frequency deviation $-\hat{\omega}_j$ via the transfer function below

$$G_j(s) = K_j \frac{1}{(1 + sT_{s,j})} \frac{(1 + sT_{3,j})}{(1 + sT_{c,j})} \frac{(1 + sT_{4,j})}{(1 + sT_{5,j})} + D_j,$$

³We assume that no zero/pole cancellation occurs between $G_j(s)$ and the PI controller.

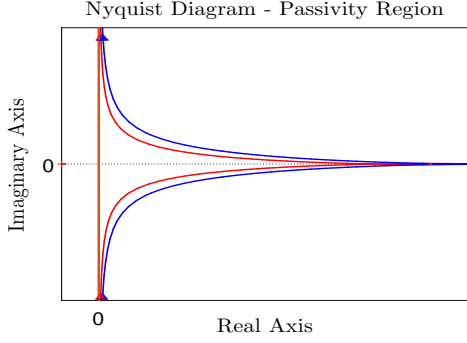


Fig. 4. Nyquist plots for the dynamics presented in (19) and (20), illustrated by blue and red lines respectively, when the described gain conditions are marginally satisfied. The passivity of both schemes is implied by the fact that both plots lie on the right half plane.

where $T_{s,j}, T_{3,j}, T_{c,j}, T_{4,j}, T_{5,j}$ are time-constants and K_j and D_j are the droop and damping coefficients respectively. Realistic values for these systems are provided by the Power System Toolbox and it can be shown that Assumption 3 is satisfied by 20 out of the 22 buses with turbine governor dynamics. Furthermore, for the remaining 2 buses, Assumption 3 is satisfied if the damping coefficients are increased by 28% and 37% respectively. This demonstrates that the passivity conditions are satisfied by existing implementations. Note that further examples of schemes that satisfy Assumption 3, including static nonlinearities, first and second order systems are provided in [9].

Remark 9: Motivated by optimality considerations, distributed control schemes have been proposed in the literature, which rely on suitable communicating variables. One such example is the distributed averaging proportional integral controller (e.g. in [26], [27]), given by

$$\gamma_j \dot{p}_j^c = -k_j \omega_j - \sum_{\{i,j\} \in E_c} a_{ij} (p_j^c - p_i^c), j \in N, \quad (21a)$$

$$p_j^M = k_j p_j^c, d_j^u = D_j \omega_j, j \in N, \quad (21b)$$

where p_j^c is the state of the controller, k_j and D_j are positive constants describing the generation gain and frequency damping, and $\gamma_j > 0$ is the time-constant of the controller at node j . The communication takes place over a connected undirected graph (N, E_c) , and the scalar $a_{ij} = a_{ji} > 0$ denotes the weight of the edge $\{i, j\} \in E_c$ indicating the strength of the communication. By synchronizing the states of the controllers and tuning the parameters k_j appropriately, frequency regulation with an optimal allocation of resources can be reached. Although our treatment does not explicitly address this class of controllers, the analysis carried out in the previous sections can be suitably modified⁴ to guarantee stability of the power network with the distributed averaging controller (21) and hysteretic load dynamics.

VII. SIMULATION ON THE NPCC 140-BUS SYSTEM

In this section we verify our analytic results with a numerical simulation on the Northeast Power Coordinating Council (NPCC) 140-bus interconnection system, using the Power System Toolbox [25]. This model is more detailed and realistic than our analytical one, including line resistances, a DC12

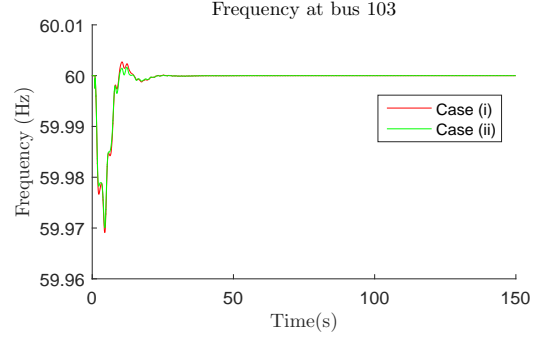


Fig. 5. Frequency at bus 103 with controllable load dynamics as in the following two cases: i) Switching case, ii) Hysteresis case.

exciter model, a subtransient reactance generator model, and turbine governor dynamics⁵.

The test system consists of 93 load buses serving different types of loads including constant active and reactive loads and 47 generation buses. The overall system has a total real power of 28.55GW. For our simulation, we added three uncontrollable loads on units 2, 8, 9, 16 and 17, each having a step increase of magnitude 3 p.u. (base 100MVA) at $t = 1$ second.

Controllable demand was considered within the simulations, with controllable loads controlled every 10ms. Additionally, generators were considered at all generation buses, with dynamics as described by (4a).

The system was tested at two different cases. In case (i), on-off controllable loads with dynamics as in (5) were included on 20 load buses. The values for $\bar{\omega}_j$ were selected from a uniform distribution within the range $[0.02 \ 0.07]$ and those of $\underline{\omega}_j$ by $\underline{\omega}_j = -\bar{\omega}_j$. Controllable loads were also included on 20 load buses for case (ii), but with dynamics described by (8). To have a fair comparison, the same frequency thresholds were used for both cases, with $\omega_j^1 = \bar{\omega}_j$ and $\omega_j^0 = \omega_j^1/4$. Also, $\bar{d} = -\underline{d} = 0.2p.u.$ was used for both cases. Cases (i) and (ii) will be referred to as the 'switching' and 'hysteresis' cases respectively.

The frequency at bus 103 for the two tested cases is shown in Fig. 5, where it can be seen that frequency returns to its nominal value for both cases, as suggested in Theorems 1 and 2. Moreover, Fig. 6 demonstrates that the inclusion of switching loads decreases the maximum overshoot in frequency, by comparing the largest deviation in frequency with and without on-off controllable loads at buses 1 – 40, where frequency overshoot was seen to be the largest. Figure 7 shows controllable demand at 4 buses for case (i), demonstrating very fast switches and indicating Zeno behavior. In contrast, when case (ii) is considered, such fast switching in loads is not observed on those 4 buses, as exhibited in Figure 8. Note that the 4 demonstrated buses where selected to be those with the minimum time between consecutive switches in the hysteretic loads of case (ii). Furthermore, both Figures 7 and 8 demonstrate times up to 10s since all loads stayed switched off afterwards. The latter demonstrates the non-disruptive nature of the two schemes, since loads return to their nominal demand after a brief period. This numerical investigation supports the analysis of this paper, verifying that hysteresis eliminates Zeno behavior at controllable loads.

⁴In particular, in the proof of Theorem 2 the term V_M needs to be replaced by $\frac{1}{2} \sum_{j \in N} (p_j^c - p_j^{c,*})^2 / \gamma_j$.

⁵The details of the simulation models can be found in the Power System Toolbox data file atanp48.

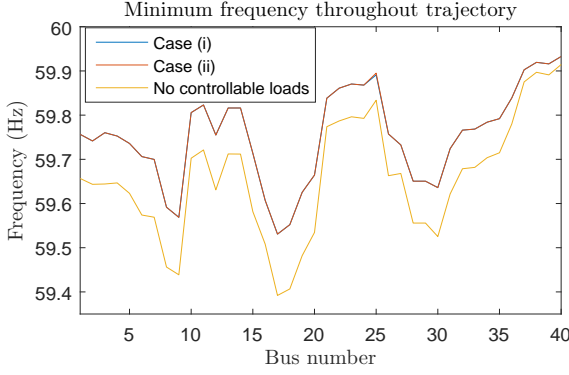


Fig. 6. Largest frequency overshoot for buses 1–40 for three cases: (i) Use of switching loads, (ii) Use of hysteresis loads, (iii) No use of controllable loads. Note that the graphs for cases (i), (ii) are almost identical and indistinguishable in the figure.

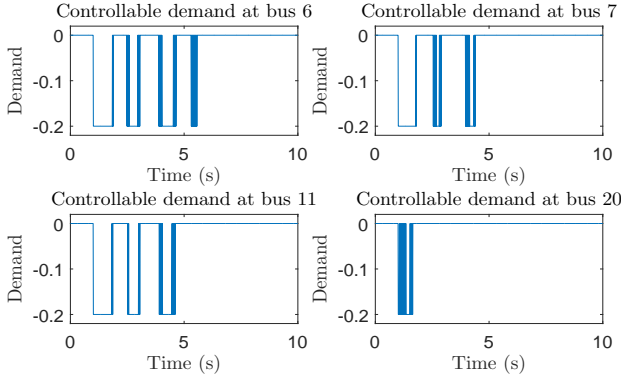


Fig. 7. Controllable demand at 4 buses with Switching on-off loads.

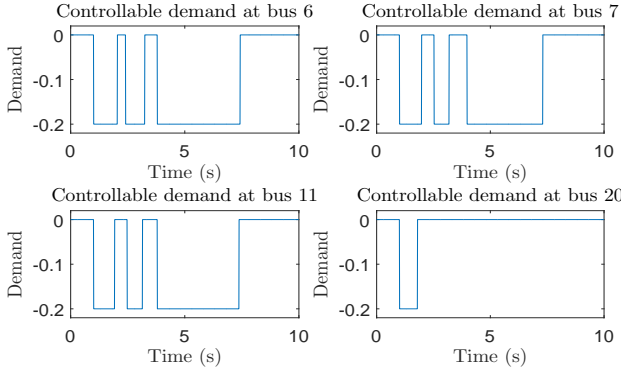


Fig. 8. Controllable demand at 4 buses with Hysteresis on-off loads.

VIII. CONCLUSION

We have considered the problem of secondary frequency control where controllable on-off loads provide ancillary services. We first considered loads that switch on when some frequency threshold is reached and off otherwise. Stability guarantees are provided for such loads. Furthermore, it is discussed that such schemes might exhibit arbitrarily fast switching, which might limit their practicality. To cope with this issue, on-off loads with hysteretic dynamics were considered. It has been shown that such loads do not exhibit any Zeno behavior and that their inclusion does not compromise power network stability. Hence, such schemes are usable for practical implementations. Both schemes ensure that controllable loads return to their nominal behavior at equilibrium and hence that disruptions occur for brief periods only. Furthermore, it has been shown that the established stability properties are retained when general passive continuous dynamics for generation and

demand are considered along with the hysteretic loads. The latter allows a broad range of highly relevant dynamics to be included in the analysis and highlights the applicability of our results. Numerical simulations on the NPCC 140-bus system verify our main findings, demonstrating that the presence of on-off loads reduces the frequency overshoot and that hysteresis schemes resolve issues caused by Zeno-like behavior. Interesting potential extensions in the analysis include incorporating frequency dependent on-off loads within the primary frequency control timeframe, more advanced load dynamics, and models that take into account voltage dynamics.

REFERENCES

- [1] A. Kasis, N. Monshizadeh, and I. Lestas, "Secondary frequency control in power networks with on-off load side participation," in *56th IEEE Conf. on Decision and Control (to appear)*, 2017.
- [2] H. Lund, "Large-scale integration of optimal combinations of pv, wind and wave power into the electricity supply," *Renewable energy*, vol. 31, no. 4, pp. 503–515, 2006.
- [3] A. Ipakchi and F. Albuyeh, "Grid of the future," *IEEE power and energy magazine*, vol. 7, no. 2, pp. 52–62, 2009.
- [4] P. Kundur, N. J. Balu, and M. G. Lauby, *Power system stability and control*, vol. 7. McGraw-hill New York, 1994.
- [5] A. Ulbig, T. S. Borsche, and G. Andersson, "Impact of low rotational inertia on power system stability and operation," *IFAC Proceedings Volumes*, vol. 47, no. 3, pp. 7290–7297, 2014.
- [6] A. Molina-Garcia, F. Bouffard, and D. S. Kirschen, "Decentralized demand-side contribution to primary frequency control," *IEEE Transactions on Power Systems*, vol. 26, no. 1, pp. 411–419, 2011.
- [7] S. Trip and C. De Persis, "Optimal generation in structure-preserving power networks with second-order turbine-governor dynamics," in *European Control Conference*, pp. 916–921, 2016.
- [8] C. Zhao, U. Topcu, N. Li, and S. H. Low, "Design and stability of load-side primary frequency control in power systems," *IEEE Transactions on Automatic Control*, vol. 59, no. 5, pp. 1177–1189, 2014.
- [9] A. Kasis, E. Devane, C. Spanias, and I. Lestas, "Primary frequency regulation with load-side participation Part I: stability and optimality," *IEEE Transactions on Power Systems*, vol. 32(5), pp. 3505–3518, 2017.
- [10] E. Devane, A. Kasis, M. Antoniou, and I. Lestas, "Primary frequency regulation with load-side participation Part II: beyond passivity approaches," *IEEE Transactions on Power Systems*, vol. 32, no. 5, pp. 3519–3528, 2017.
- [11] E. Mallada, C. Zhao, and S. Low, "Optimal load-side control for frequency regulation in smart grids," in *52nd Annual Allerton Conference on Communication, Control, and Computing*, pp. 731–738, 2014.
- [12] S. Trip, M. Bürger, and C. De Persis, "An internal model approach to (optimal) frequency regulation in power grids with time-varying voltages," *Automatica*, vol. 64, pp. 240–253, 2016.
- [13] A. Kasis, E. Devane, and I. Lestas, "Stability and optimality of distributed schemes for secondary frequency regulation in power networks," in *55th IEEE Conf. on Decision and Control*, pp. 3294–3299, 2016.
- [14] T. Liu, D. J. Hill, and C. Zhang, "Non-disruptive load-side control for frequency regulation in power systems," *IEEE Transactions on Smart Grid*, vol. 7, no. 4, pp. 2142–2153, 2016.
- [15] R. Goebel, R. G. Sanfelice, and A. R. Teel, "Hybrid dynamical systems," *IEEE Control Systems Magazine*, vol. 29, no. 2, pp. 28–93, 2009.
- [16] J. Cortés, "Discontinuous dynamical systems," *IEEE Control Systems Magazine*, vol. 28, no. 3, 2008.
- [17] T. Tao, *An introduction to measure theory*, vol. 126. American Mathematical Soc., 2011.
- [18] A. R. Bergen and V. Vittal, *Power Systems Analysis*. Prentice Hall, 1999.
- [19] S. Hu, "Differential equations with discontinuous right-hand sides," *Journal of Mathematical Analysis and Applications*, vol. 154, no. 2, pp. 377–390, 1991.
- [20] F. Dörfler, M. Chertkov, and F. Bullo, "Synchronization in complex oscillator networks and smart grids," *Proceedings of the National Academy of Sciences*, vol. 110, no. 6, pp. 2005–2010, 2013.
- [21] H. Lee and V. I. Utkin, "Chattering suppression methods in sliding mode control systems," *Annual reviews in control*, vol. 31, no. 3, 2007.
- [22] C. G. Mayhew, R. G. Sanfelice, and A. R. Teel, "Quaternion-based hybrid control for robust global attitude tracking," *IEEE Transactions on Automatic Control*, vol. 56, no. 11, pp. 2555–2566, 2011.
- [23] F. Ceragioli, C. De Persis, and P. Frasca, "Discontinuities and hysteresis in quantized average consensus," *Automatica*, vol. 47, no. 9, pp. 1916–1928, 2011.
- [24] H. K. Khalil, *Nonlinear systems*, vol. 3. Prentice Hall New Jersey, 1996.
- [25] K. Cheung, J. Chow, and G. Rogers, "Power system toolbox, v 3.0," *RPI and Cherry Tree Scientific Software*, 2009.
- [26] F. Dörfler, J. W. Simpson-Porco, and F. Bullo, "Plug-and-play control and optimization in microgrids," in *53rd IEEE Conf. on Decision and Control*, pp. 211–216, 2014.

- [27] F. Dörfler, J. Simpson-Porco, and F. Bullo, "Breaking the hierarchy: distributed control & economic optimality in microgrids," *IEEE Transactions on Control of Network Systems*, vol. 3, no. 3, pp. 241–253, 2015.
- [28] A. Bacciotti and F. Ceragioli, "Stability and stabilization of discontinuous systems and nonsmooth lyapunov functions," *ESAIM: Control, Optimisation and Calculus of Variations*, vol. 4, pp. 361–376, 1999.
- [29] R. G. Sanfelice, R. Goebel, and A. R. Teel, "Invariance principles for hybrid systems with connections to detectability and asymptotic stability," *IEEE Transactions on Automatic Control*, vol. 52, no. 12, pp. 2282–2297, 2007.

Supplementary material

A. PROOFS OF RESULTS

In this section we provide the proofs of the lemmas and theorems stated in this paper.

Within the proofs of Lemma 1 and Theorem 1 we will make use of the following equilibrium equations for system (3)–(4), which follow from Definition 1 and Lemma 1. Below, we let $\bar{N} \subseteq N$ be the set of all buses with non-trivial generation dynamics, i.e. those where $\alpha_j > 0$ in (4a).

$$0 = \omega_i^* - \omega_j^*, \quad (i, j) \in E, \quad (22a)$$

$$0 = -p_j^L + p_j^{M,*} - \sum_{k:j \rightarrow k} p_{jk}^* + \sum_{i:i \rightarrow j} p_{ij}^*, \quad j \in N, \quad (22b)$$

$$p_{ij}^* = B_{ij} \sin \eta_{ij}^*, \quad (i, j) \in E, \quad (22c)$$

$$0 = \omega_j^*, \quad j \in \bar{N}, \quad (22d)$$

$$0 = d_j^{c,*}, \quad j \in N. \quad (22e)$$

Proof of Lemma 1: The result follows from equilibrium equations (22a) and (22d). Note that $\omega^* = \mathbf{0}_{|N|}$ implies that $d^{u,*} = d^{c,*} = \mathbf{0}_{|N|}$ from (4b) and (5) respectively. ■

Proof of Lemma 2: Noting that the vector field is piecewise continuous, we use Proposition 5 in [16] to establish existence and uniqueness of solutions. To this end, observe that at any point of discontinuity one of the following holds:

- (i) The vector fields point in the same direction.
- (ii) The vector fields point towards the discontinuity.

In fact, at a point of discontinuity, say $\omega_j = \bar{\omega}_j$, we have $\dot{\omega}|_{d_j^c = \bar{d}_j} \leq \dot{\omega}|_{d_j^c = 0}$. This rules out the case where the vector field points away from the discontinuity from both sides. An analogous argument can be made for the case $\omega_j = \underline{\omega}_j$. Consequently, whenever the solution reaches a point of discontinuity it will either continue in the same direction (as in (i)) or stay there (as in (ii)) and therefore existence and uniqueness of solutions follow from [16, Prop. 5]. ■

Proof of Theorem 1: We will use the dynamics in (3) and (4) to define a Lyapunov function for system (3)–(5).

First, consider $V_F(\omega) = \frac{1}{2} \sum_{j \in N} M_j \omega_j^2$. By substituting (3b) for $\dot{\omega}_j$ and using the differential inclusion for d_j^c for $j \in N$, the time-derivative along solutions of (3)–(5) is then obtained as

$$\dot{V}_F = \left\{ \sum_{j \in N} \omega_j (-p_j^L + p_j^M - v_j - d_j^u) - \sum_{k:j \rightarrow k} p_{jk} + \sum_{i:i \rightarrow j} p_{ij} : v_j \in F[d_j^c(\omega_j)] \right\}.$$

Here, \dot{V}_F has to be interpreted as the set-valued derivative of V_F with respect to (3)–(5). By (22), it is easy to observe that

$$\dot{V}_F = \left\{ \sum_{(i,j) \in E} (p_{ij} - p_{ij}^*)(\omega_j - \omega_i) + \sum_{j \in N} \omega_j (p_j^M - p_j^{M,*} - v_j - d_j^u) : v_j \in F[d_j^c(\omega_j)] \right\}. \quad (23)$$

Additionally, consider $V_P(\eta) = \sum_{(i,j) \in E} B_{ij} \int_{\eta_{ij}^*}^{\eta_{ij}} (\sin \phi - \sin \eta_{ij}^*) d\phi$. Using (3a) and (3c), the time-derivative equals

$$\begin{aligned} \dot{V}_P &= \sum_{(i,j) \in E} B_{ij} (\sin \eta_{ij} - \sin \eta_{ij}^*)(\omega_i - \omega_j) \\ &= \sum_{(i,j) \in E} (p_{ij} - p_{ij}^*)(\omega_i - \omega_j). \end{aligned} \quad (24)$$

Finally, consider the function $V_M(p^M) = \frac{1}{2} \sum_{j \in N} (p_j^M - p_j^{M,*})^2$. Using (4a), its time derivative is given by

$$\dot{V}_M = \sum_{j \in N} (p_j^M - p_j^{M,*})(-\omega_j), \quad (25)$$

noting that $p_j^M = p_j^{M,*}$ for each $j \in N/\bar{N}$. Based on the above, we define the function

$$V(\eta, \omega, p^M) = V_F(\omega) + V_P(\eta) + V_M(p^M). \quad (26)$$

By (4b) and (23)–(25), we have

$$\dot{V} = \left\{ \sum_{j \in N} (-\omega_j v_j - A_j(\omega_j)^2) : v_j \in F[d_j^c(\omega_j)] \right\}. \quad (27)$$

Using (6), we conclude that

$$\max \dot{V} \leq - \sum_{j \in N} A_j(\omega_j)^2 \leq 0, \quad (28)$$

where the maximum is taken over all the points in the set given by the right hand side of (27).

Clearly V_F and V_M have strict global minima at $\omega = \omega^* = 0$ and $p^M = p^{M,*}$ respectively. Additionally, Assumption 1 guarantees the existence of some neighborhood of each η_{ij}^* on which the respective integrand in the definition of V_P is increasing. Since the integrand is zero at the lower limit, η_{ij}^* , this immediately implies that V_P has a strict local minimum at η^* . Thus, V has a strict local minimum at the point $x^* := (\eta^*, \omega^*, p^{M,*})$. We can thus choose a neighborhood in the coordinates (η, ω, p^M) about x^* which is a strict minimum of V . From (28), within this neighborhood, V is a non-increasing function of all states and has a strict local minimum at x^* . Consequently, the connected component of the level set $\{(\eta, \omega, p^M) : V \leq \epsilon\}$ containing x^* is both compact and positively invariant with respect to (3)–(5) for sufficiently small $\epsilon > 0$. Hence, there exists a compact positively invariant set Ξ for (3)–(5) containing x^* .

Therefore, Theorem 3 in [28] can be invoked for the function V on the compact and positively invariant set Ξ along solutions of (7). This guarantees that all solutions of (3)–(5) with initial conditions $(\eta(0), \omega(0), p^M(0)) \in \Xi$ converge to the largest invariant set within $\Xi \cap \{(\eta, \omega, p^M) : 0 \in \dot{V}\}$. Note that $0 \in \dot{V}$ only if $\omega = \omega^* = \mathbf{0}_{|N|}$, which also implies that $d^c = d^u = \mathbf{0}_{|N|}$. This suggests from (3a) and (4a) that

the vectors η and p^M are equal to some constant vectors $\bar{\eta}$ and \bar{p}^M , on the invariant set. Therefore, we conclude by [28, Thm. 3] that all Filippov solutions of (3)–(5) with initial conditions $(\eta(0), \omega(0), p^M(0)) \in \Xi$ converge to the set of equilibria defined in Definition 1. This completes the proof. ■

Proof of Lemma 3: Recall that any equilibrium z^* of (12) satisfies $f(z^*) = 0, z^* \in C$ or $g(z^*) = z^*, z^* \in D$. The latter case is excluded since $g(z) : D \rightarrow C$. Therefore, $z^* \in C$. From equations (9a) and (9d) at equilibrium, it follows that $\omega^* = \mathbf{0}_{|N|}$, which implies that $\sigma_j = \mathbf{0}_{|N|}$. ■

Proof of Lemma 4: To show the existence and uniqueness of solutions, first note that for any initial condition it holds that either $z(0, 0) \in C$ or $z(0, 0) \in D$. The latter results in $z(0, 1) \in C$ as $g(z) : D \rightarrow C$. Then, from the continuity and the Lipschitz property of the dynamics in (9), it follows that a solution exists for t sufficiently close to 0, and is unique. Given $z(0, \ell) \in C$, let $\bar{t} > 0$ be the minimal time such that the solution remains within C . If $\bar{t} = \infty$ then we have concluded the argument. Otherwise there exists $\tau \geq \bar{t}$ such that the solution exists within $T_\ell = [0, \tau)$ and it holds that $z(\tau, \ell + 1) = g(z(\tau, \ell))$, where $z(\tau, \ell) \in D$ and $z(\tau, \ell + 1) \in C$. After this transition the solution can be uniquely extended starting from $z(\tau, \ell + 1) \in C$ by repeating the above argument. The solution $z(t, \ell)$ is unique since it results from the concatenation of unique solutions of (9) and (11).

To show that any maximal solution z is complete, first let t_ℓ be the time instant where the ℓ^{th} transition occurs, and then consider the time domain K of z and assume that K is bounded. Then there exist finitely many intervals of the form $[t_\ell, t_{\ell+1}] \times \{\ell\}$ with the last interval either $[t_\ell, t_{\ell+1}] \times \{\ell\}$ or $[t_\ell, t_{\ell+1}] \times \{\ell\}$ with $t_{\ell+1} < \infty$. From the global Lipschitz property of the vector field in (9), we have, however, that if no discrete transition occurs in the last interval the solution is defined for all $t > t_\ell$. Thus, since $t_{\ell+1} < \infty$ we have that a transition occurs at $t_{\ell+1}$ and therefore the solution z is not maximal. Hence, all maximal solutions are complete by contradiction. ■

Proof of Proposition 1: Consider any bounded solution of the system (12) with states $z = (\eta, \omega, p^M, \sigma)$ and define $\epsilon_j = \omega_j^1 - \omega_j^0$ following the description in (8). For any finite time interval between two consecutive switches at bus j , i.e. $[t_{\ell,j}, t_{\ell+1,j}]$, the value of $\dot{\omega}_j$ is bounded from above by a constant, say $d\omega_j^{\max}$. The fact that $d\omega_j^{\max}$ is finite follows from boundedness of the solution and the fact that the vector field in (9) is globally Lipschitz. Then, it follows that $t_{\ell+1,j} - t_{\ell,j} \geq \epsilon_j / d\omega_j^{\max}$. Notice that the condition provided in the lemma is stated from the second switching time to include the case $z(0) \in D$. ■

Proof of Theorem 2: For the proof we shall make use of the function V , described by (26). Using similar arguments as in the proof of Theorem 1 and defining $T_c = \{t : (t, \ell) \in K, z(t, \ell) \in C\}$, $T_d = \{t : (t, \ell) \in K, z(t, \ell) \in D\}$ it follows that

$$\dot{V} \leq - \sum_{j \in N} A_j (\omega_j)^2, t \in T_c \quad (29a)$$

$$V(g(z)) - V(z) = 0, t \in T_d, \quad (29b)$$

along any solution of (12). Note that when $z \in D$, the value of V remains constant as it only depends on x that is constant from (11).

Note that V is a function of x only, and is nonnegative for all x in a neighbourhood of the equilibrium x^* . Moreover,

$V = 0$ yields $\omega = \omega^* = 0$, and thus $\sigma = \sigma^* = 0$. Hence, the function V serves as a Lyapunov function for the hybrid system (12a). Then there exists a compact and positively invariant set $S = \{(x, \sigma) : x \in \Xi \text{ and } \sigma \in \bar{\mathcal{I}}(\omega)\}$ for some neighbourhood Ξ of x^* . Note that the positively invariant set Ξ is obtained in the same vein as in the proof of Theorem 1, and that the set $\{(x, \sigma) : \sigma \in \bar{\mathcal{I}}(\omega)\}$ is positively invariant by construction. Recall that, by Lemma 4 and Proposition 1, solutions of (12a) are unique, complete, and the time interval between any two consecutive switches of individual loads is bounded from below by a positive number. Therefore, by [15], [29], there exists $r > 0$ such that solutions to (12) converge to the largest (weakly) invariant subset⁶ of the set $\{z : V(z) = r\} \cap \{z \in C : \dot{V} = 0\} \cap S$. The characterization of this invariant set follows in a similar way as in the proof of Theorem 1, noting that the equilibria of (12) are as described by Lemma 3. ■

Proof of Lemma 5: From Assumption 2 and (22a) it follows that $\omega^* = \mathbf{0}_{|N|}$. Then, from (8) it follows that $\sigma^* = \mathbf{0}_{|N|}$. Consequently, and using (10), it follows that $z^* \in C$. ■

Proof of Theorem 3: From Assumption 3, it follows that within neighbourhoods Ω_j and X_j^s of $-\omega_j^*$ and $x_j^{s,*}$ respectively it holds that

$$\dot{V}_j^S(x_j^s) \leq (-\omega_j)(s_j - s_j^*) - \phi_j(-\omega_j), j \in N, \quad (30)$$

noting that $\omega^* = \mathbf{0}_{|N|}$ follows from Lemma 5. Now recall the functions V_F and V_P described in the proof of Theorem 1 and consider the candidate Lyapunov function

$$V(\eta, \omega, x^s) = V_F(\omega) + V_P(\eta) + \sum_{j \in N} V_j^S(x_j^s). \quad (31)$$

Using (23), (24) and (30), it follows that when $-\omega_j \in \Omega_j, x_j^s \in X_j^s, j \in N$, then

$$\dot{V} \leq - \sum_{j \in N} \phi_j(\omega_j)^2, t \in T_c \quad (32a)$$

$$V(g(z)) - V(z) = 0, t \in T_d, \quad (32b)$$

along the solutions of (17), where T_c and T_d are as defined in the proof of Theorem 2.

As described in the proof of Theorem 1, V_F and V_P have local minima at $\omega = \omega^* = \mathbf{0}_{|N|}$ and $\eta = \eta^*$ respectively. Also, by Assumption 3, it follows that V_j^S has a strict minimum at $x_j^{s,*}, j \in N$. Hence, V has a local strict minimum at $x^* = (\eta^*, \omega^*, x^{s,*})$. We now consider a neighbourhood of x^* where it holds that $(-\omega_j) \in \Omega_j, x_j^s \in X_j^s, j \in N$. Within this neighbourhood V is decreasing and therefore the connected component of the level set $\{(\eta, \omega, x^s) : V \leq \epsilon\}$ containing x^* is both compact and positively invariant with respect to (17) for sufficiently small $\epsilon > 0$.

The convergence proof then follows analogously to the proof of Theorems 1 and 2, noting that the invariant set, where $\omega^* = \mathbf{0}_{|N|}$, comprises only of equilibria of the system (17) by assumption. This completes the proof. ■

B. HYBRID TIME DOMAIN AND SOLUTIONS

In this section we provide for completeness a detailed definition of what is meant by a solution $z(t, \ell)$ of a hybrid

⁶We use the notion of invariant sets provided in [29]. The distinction between “weak” and “strong” invariant sets is unnecessary in this case as solutions of (12) are unique by Lemma 4.

system of the form (12), and a definition of its corresponding hybrid time domain.

Definition 3 ([15]): A hybrid time domain is a subset of $\mathbb{R}_{\geq 0} \times \mathbb{N}_0$ consisting of, potentially infinite, time intervals of the form $[t_\ell, t_{\ell+1}] \times \{\ell\}$, where $0 = t_0 \leq t_1 \leq \dots$, or of finitely many such intervals with the last one possibly of the form $[t_\ell, t_{\ell+1}] \times \{\ell\}$, $[t_\ell, t_{\ell+1}) \times \{\ell\}$ or $[t_\ell, \infty) \times \{\ell\}$. Consider a function $z(t, \ell)$ defined on a hybrid time domain K such that for every fixed ℓ , $t \rightarrow z(t, \ell)$ is a locally absolutely continuous function on the interval $T_\ell = \{t : (t, \ell) \in K\}$. The function $z(t, \ell)$ is a solution to (12) if $z(0, 0) \in \Lambda_0$ and for each ℓ it holds that

$$\begin{aligned} \dot{z}(t, \ell) &= f(z(t, \ell)), \text{ for almost all } t \in T_\ell, \\ z(t, \ell) &\in C, \text{ for all } t \in [\min T_\ell, \sup T_\ell), \\ z(t, \ell + 1) &= g(z(t, \ell)), \text{ } z(t, \ell) \in D \\ &\text{for all } (t, \ell) \in K \text{ such that } (t, \ell + 1) \in K. \end{aligned}$$

A solution $z(t, \ell)$ is complete if K is unbounded. A solution is maximal if it cannot be extended (i.e., there is no other solution \tilde{z} with time domain \tilde{K} such that K is a proper subset of \tilde{K} and \tilde{z} agrees with z on K).